Food-grade titanium dioxide translocates across the oral mucosa in pigs and induces genotoxicity in an in vitro model of human oral epithelium

Julien Vignard, Aurélie Pettes-Duler, Eric Gaultier, Christel Cartier, L. Weingarten, A. Biesemeier, T. Taubitz, Philippe Pinton, C. Bebeacua, Laurent Devoille, et al.

Food-grade titanium dioxide translocates across the oral mucosa in pigs and induces genotoxicity in an in vitro model of human oral epithelium

J Vignard
Toxalim UMR1331 (Research Centre in Food Toxicology), Toulouse University, INRAE, ENVT, INP-Purpan, UPS, Toulouse

A Pettes-Duler
Toxalim UMR1331 (Research Centre in Food Toxicology), Toulouse University, INRAE, ENVT, INP-Purpan, UPS, Toulouse

E Gaultier
Toxalim UMR1331 (Research Centre in Food Toxicology), Toulouse University, INRAE, ENVT, INP-Purpan, UPS, Toulouse

C Cartier
Toxalim UMR1331 (Research Centre in Food Toxicology), Toulouse University, INRAE, ENVT, INP-Purpan, UPS, Toulouse

L Weingarten
Centre de MicroCaractérisation Raimond Castaing, UAR 3623, Toulouse

A Biesemeier
Luxembourg Institute of Science and Technology (LIST), Materials Research and Technology (MRT), Advanced Instrumentation for Ion Nano-Analytics (AINA), L-4362 Esch-sur-Alzette

T Taubitz
Luxembourg Institute of Science and Technology (LIST), Materials Research and Technology (MRT), Advanced Instrumentation for Ion Nano-Analytics (AINA), L-4362 Esch-sur-Alzette

P Pinton
Toxalim UMR1331 (Research Centre in Food Toxicology), Toulouse University, INRAE, ENVT, INP-Purpan, UPS, Toulouse

C Bebeacua
ETH Zurich, ScopeM, Otto-Stern-Weg 3, 8093 Zurich

L Devoille
Department of materials, LNE, Trappes

J Dupuy
Toxalim UMR1331 (Research Centre in Food Toxicology), Toulouse University, INRAE, ENVT, INP-Purpan, UPS, Toulouse

E Boutet-Robinet

Toxalim UMR1331 (Research Centre in Food Toxicology), Toulouse University, INRAE, ENVT, INP-Purpan, UPS, Toulouse

N Feltin

Department of materials, LNE, Trappes

IP Oswald

Toxalim UMR1331 (Research Centre in Food Toxicology), Toulouse University, INRAE, ENVT, INP-Purpan, UPS, Toulouse

FHF Pierre

Toxalim UMR1331 (Research Centre in Food Toxicology), Toulouse University, INRAE, ENVT, INP-Purpan, UPS, Toulouse

B Lamas

Toxalim UMR1331 (Research Centre in Food Toxicology), Toulouse University, INRAE, ENVT, INP-Purpan, UPS, Toulouse

G Mirey

Toxalim UMR1331 (Research Centre in Food Toxicology), Toulouse University, INRAE, ENVT, INP-Purpan, UPS, Toulouse

E Houdeau (✉ eric.houdeau@inrae.fr)

Toxalim UMR1331 (Research Centre in Food Toxicology), Toulouse University, INRAE, ENVT, INP-Purpan, UPS, Toulouse

---

Research Article

Keywords: Oral mucosa, titanium dioxide, food additive, nanoparticles, cytotoxicity, genotoxicity

Posted Date: July 5th, 2022

DOI: https://doi.org/10.21203/rs.3.rs-1788223/v1

Abstract

Background

Food-grade titanium dioxide (TiO_2), composed of nano- and submicron-sized particles, is used worldwide in various foodstuffs, toothpastes and pharmaceutical tablets as a whitening and opacifying agent. Its use as a food additive (E171 in EU) has raised concerns for human health regarding its systemic availability, tissue accumulation, genotoxicity and promotion of precancerous lesions. However, although the buccal mucosa is the first area exposed, oral transmucosal passage of TiO_2 particles has not been documented. Here we analyzed TiO_2 (E171) particle translocation *in vivo* through the pig buccal mucosa and *in vitro* on human buccal TR146 cells, and the effects of E171 on proliferating and differentiated human oral epithelial cells.

Results

Using transmission electronic microscopy (TEM) coupled to energy-dispersive X-ray spectroscopy (EDX), isolated TiO_2 particles and small aggregates were observed in the buccal floor of pigs starting 30 min after the sublingual deposition of E171 suspended in water, and recovered in the submandibular lymph nodes at 4 h. In human TR146 cells exposed to E171, kinetic analyses using confocal microscopy, TEM and high-resolution secondary ion mass spectrometry (SIMS) imaging showed high uptake capacities of both the nano- and submicron-sized TiO_2 particles. At 2 h, the cytotoxicity, genotoxicity and oxidative stress were investigated in both proliferating and differentiated TR146 cells exposed to E171 in comparison with two TiO_2 size standards of 115 and 21 nm in diameter. All TiO_2 samples were reported cytotoxic in proliferating cells, an effect almost abolished following differentiation. Genotoxicity (γH2AX or 53BP1 foci formation and comet assays) and oxidative stress (CellRox reagent) were only reported for the E171 and 115 nm TiO_2 particles, and mainly in proliferating cells.

Conclusions

These data showed that the buccal mucosa is an important absorption route for the systemic passage of food-grade TiO_2 particles. In human cells, TiO_2 particles are cytotoxic and generate size-dependent oxidative and genotoxic stresses in proliferating cells, potentially impairing oral epithelium renewal. Altogether, these data emphasize that buccal exposure should be considered during toxicokinetic studies and for risk assessment of TiO_2 in human when used as food additive, including in toothpastes and pharmaceutical formulations.

Introduction

Due to the rapid expansion of nanotechnologies and the daily increasing use of nanomaterials in consumer products, there is a growing need to assess the toxicological risks of these materials on human health. Such concern increases when nanoparticles (NPs) are found in food additives and coating substances or are included in food packaging, leading to chronic oral exposure to NPs for consumers. Among these agents, food-grade titanium dioxide (TiO_2) is commonly used as a food additive worldwide, and is referred to as E171 in European Union. It is used *ad quantum satis* as a whitening and brightening agent in a variety of food products (confectionary and bakery commodities, white sauces and icing), as beverage whiteners and in personal care products such as toothpaste and pharmaceutical tablets [1–3]. For these uses, large amounts of TiO_2 powders are produced and are composed of particles of various sizes ranging from 20 to 400 nm, and up to 55% of them by number are NPs (diameter < 100 nm) [4–7]. Focusing on only food origin, depending on the exposure scenario and population groups, the mean dietary intake in humans has been estimated to range from 0.03 mg of TiO_2/kg of body weight (bw)/ day (d) in infants to 11.5 mg/kg bw/d in children under 10 years of age and up to 6.7 mg/kg bw/d for older groups [8]. Concerning TiO_2 fate and organ toxicity, chronic exposure to TiO_2 has been reported to result in particle accumulation in human tissues, including the intestine, liver, spleen and kidney [9, 10] as well as in the placenta [7]. Investigations in rodent models and cell lines have raised concerns regarding genotoxicity, inflammation and oxidant-antioxidant imbalance [1] as well as the potential for E171 to initiate and promote preneoplastic lesions in the rat colon [6, 11]. In mice, daily exposure to food-grade TiO_2 in a colitis-associated colorectal cancer model also exacerbated tumour formation in the colon [12].

To date, risk assessments of TiO_2 by food and consumer product safety authorities has mainly been based on the assumption that orally ingested TiO_2-NPs are mainly absorbed by the intestine [8, 13, 14]. However, oral toxicokinetic studies have estimated that only 0.02–0.6% of the administered TiO_2 dose is absorbed at the intestinal level including in humans [14–17]. When considering the oral uptake of xenobiotics, the buccal cavity represents the first area of exposure and thus the first possible systemic delivery portal. In the context of food additives, the cellular uptake and toxicity potential of food-grade TiO_2 has not been addressed in a buccal model, although the mouth should be considered to be the body region exposed to a higher load of TiO_2-NPs once they are released from the food matrix. Indeed, with the example of chewing gum, among other sweets in which TiO_2 is used as a surface colouring agent [18, 19], TiO_2 particles may be easily released from the gum [18, 20], dispersed in the saliva, and rapidly come into contact with the buccal epithelium before being swallowed. Similar scenarios can be drawn in other food categories where TiO_2 is added to a liquid or semiliquid matrix including ice cream, sauces and drinks [8], or when used as an opacifier in pharmaceutical tablets coating formulations [2].

Given the lack of information on the food additive E171, the potential of toxicity of TiO_2 at the mouth level has been addressed in few studies using NP models of known sizes. In a porcine *ex vivo* model of the buccal cavity exposed to nanomodels, five TiO_2-NPs with distinct physicochemical properties were shown to permeate the mucosa layer and penetrate the oral epithelium [21, 22]. Mucosal penetration and intracellular outcome depend on particle size and surface hydrophilicity/hydrophobicity. Indeed, TiO_2

penetrated the entire buccal epithelium and the connective tissue, except for the nanomaterials with the smallest particle size, which were unable to reach the lower epithelium. Such size-dependent permeation into the deeper part of the buccal mucosa has already been observed for the penetration of neutral polystyrene NPs [23]. Moreover, hydrophilic TiO_2-NPs appeared to be freely distributed in the cytoplasm as small aggregates whereas their hydrophobic counterparts were encapsulated into vesicle structures. Regardless of their cellular distribution, none of the tested TiO_2-NPs were shown to affect cell viability or membrane integrity in the TR146 human buccal cell line, even under different levels of oxidative stress, which might depend on the physicochemical properties of the particles. Nonetheless, this evaluation remains to be investigated with the food form of TiO_2 for risk assessment purposes given the mixed composition of nano- and submicron-sized particles in commercial batches.

The median turnover of the buccal mucosa is 14 days [21], implying active stem cell division to ensure epithelium renewal. Therefore, in the context of oral exposure, it is important to take into account the role of the cell cycle when assessing particle toxicity. To gain insight into the possible toxic effects of food-grade TiO_2 at the mouth level, the translocation of TiO_2 particles from the food additive E171 was first assessed *in vivo* in piglet mouths, for which the histomorphology of the buccal mucosa is comparable to that of humans. Second, we used the human TR146 cell line, either in cycling or noncycling differentiated cells, as a model of the buccal mucosa composed of cells with different proliferation statuses. The kinetic of the cellular permeability to foodborne TiO_2 particles, as well as cytotoxicity, genotoxicity and oxidative stress in TR146 cells exposed to the food additive were evaluated. Due to the wide particle size distributions in food-grade TiO_2 powders, a comparative toxicity study was also performed with two TiO_2 particle models with distinct primary sizes.

Materials And Methods

Chemicals and particle preparation

Food-grade TiO_2 (E171) was purchased as a powder from the website of a French commercial supplier of food colouring agents and was previously characterized as a representative E171 sample in the anatase crystal form that has been placed on the EU market [7]. Two other (anatase) TiO_2 test materials with distinct primary particle sizes were used in this study, namely 21 nm TiO_2-NP (Sigma–Aldrich, Saint-Quentin-Fallavier, France) and 115 nm TiO_2, referenced to JRC10200a by the European Joint Research Center Nanomaterials Repository (JRC, Ispra, Italy). All TiO_2 materials were sonicated in ultrapure water (1 mg/ml) placed in an ice bath for 1 min at 40% amplitude (VCX 750 – 230 V, Sonics Materials) to obtain a stable dispersion of TiO_2 particles and then stored at 4°C during 15 days maximum before use. Dynamic light scattering (DLS; Zetasizer Nano ZS; Malvern Instruments Ltd.) measurements were performed on each TiO_2 material in ultrapure water (pH = 7.75) and in TR146 cell culture medium (Ham's F12, pH 7.54; Life Technologies, Illkirch, France). Ten microlitres of E171, TiO_2 JRC10200a or TiO_2-NP suspensions

were diluted in 2 mL of ultrapure water or Ham's F12 medium, and the hydrodynamic diameter (Z-average), polydispersity index and zeta potential were measured.

Animals and study design for in vivo buccal exposure

Five 4-week-old weaned castrated male piglets (Pic 410) weighing 10–12 kg were obtained from a local swine supplier (Gaec de Calvignac, Saint-Vincent d'Autejac, France). All animal studies were carried out in accordance with the European Guidelines for the Care and Use of Animals for Research Purposes (Directive 2010/63/EU) and validated by the Ethics Committee for Animal Experiments Toxcomethique n° 86 (TOXCOM/121/LGU). Pigs were acclimatized for 1 week in the animal facility of the INRAE Research Centre in Food Toxicology (Toxalim, Toulouse, France) and fed *ad libitum* with free access to water. One pig served as a control, being administered water free from the food additive, and the other 4 pigs were exposed to TiO_2 (E171) water suspension, dispersed (n = 2) or not (n = 2) by sonication. During a short restraint operated by an animal technician, a volume of 200 µl of food-grade TiO_2 (E171) suspension dispersed in water (50 µg/ml) was gently deposited once at T0 in the mouth under the tongue using a syringe equipped with a flexible catheter to avoid any injury in the mouth. The same procedure was repeated at T0 + 1, 2 and 3 h, and animals were euthanized at T0 + 30 min (n = 2) or at T0 + 4 h, i.e., one hour after the last sublingual deposit (n = 3, including the control pig). During the exposure period, all piglets were allowed to move freely in the barn without access to water or feed to avoid dilution in the mouth. At sacrifice, tissue samples from the buccal cavity under the tongue (buccal floor) as well as the submandibular lymph nodes located underneath the tongue were quickly withdrawn and prepared for TEM analysis.

Buccal tissue preparation for TEM-EDX analysis

Tissue samples from piglets were fixed in 2.5% paraformaldehyde-2.5% glutaraldehyde in 0.1 M cacodylate buffer (pH 7.4) overnight at 4°C. After several rinses with cacodylate buffer, the samples were postfixed in 1% OsO_4 (Osmium (VIII) oxide) for 1 h (4°C) and then rinsed again with cacodylate buffer before being dehydrated using a graded series of ethanol. The sections were impregnated in low viscosity epoxy resin (EMS) under vacuum and then polymerized at 60°C for 48–72 h. Ultrathin sections (80 nm, Ultracut UCT, Leica) were collected on copper grids and stained with a UAR-EMS (uranyl acetate replacement) solution followed by a 0.4% lead citrate solution. Five to 6 tissue sections from each sample were observed under a JEOL JEM-1400 electron microscope (MeTi facility, Toulouse, France) operated at 200 kV for TEM observations of electron dense particles and analysed by energy-dispersive X-ray spectroscopy (EDX) on a JEOL 2100F (Raymond Castaing facility, Toulouse, France) for chemical elemental analysis. Measurements of minimum and maximum Feret diameters were performed from bright-field TEM images by using the image processing open-source software ImageJ (NIH, United States).

Cell culture and TiO_2 treatments

Human TR146 buccal epithelial cells (Sigma–Aldrich) were cultured in Ham's F12 nutrient mix (Life Technologies) supplemented with 10% foetal bovine serum (FBS; Gibco, Life Technologies) and 0.1% penicillin/streptomycin. Cells were maintained at 37°C in a humidified atmosphere containing 5% CO_2 and subcultured every 2–3 days. To differentiate the TR146 cells, 10 000 cells were seeded in 0.33 cm^2 Transwell inserts (Corning) for 30 days, and the culture medium was changed every 2–3 days. Cells were exposed for 2 h to different concentrations of food-grade TiO_2 (E171) (5, 50 or 100 µg/ml) or to the test materials TiO_2 (JRC10200a and TiO_2-NP) in Ham's F12 without FBS and when indicated, washed twice with PBS before being incubated in fresh complete culture medium.

Confocal microscopy, TEM and SIMS imaging on TR146 cells

To study the kinetics of food-grade TiO_2 particle absorption, human epithelial TR146 cells were exposed for 1 h, 2 h, 5 h and 24 h to a 50 µl/ml suspension of TiO_2 (E171) in Ham's F12. Control cells were exposed to Ham's F12 only. Supplemental TR146 cells exposed to E171 for 2 h were rinsed with Ham's F12 before being cultivated for a 5 h wash-out period in the same culture medium free of TiO_2 particles. For confocal microscopy, TR146 cells were fixed in 4% buffered formalin, embedded in paraffin wax, and sectioned to a thickness of five microns. Sections were first incubated with WGA-Alexa 594 for 1 h in the dark and then washed before being mounted with DAPI (4',6-diamidino-2-phenylindole; Life Technologies, France)-containing ProLong Gold antifade mounting medium for fluorescence microscopy. Tissue sections were viewed under a Leica SP8 confocal microscope with a 40× immersion objective and examined at 488/BP 488–494 nm to detect laser reflection by the metal particles as previously described [24].

For TEM, TR146 cell monolayers were treated as previously described for buccal tissues. Since EDX might not be sensitive enough to allow investigation of the uptake of single NPs in cell preparations, correlative high-resolution imaging and secondary ion mass spectrometry (SIMS) were performed using a customized Zeiss Orion NanoFab helium ion microscope called the "npSCOPE" instrument [25] developed in the framework of EU HORIZON 2020 project no. 720964. TR146 cells exposed for 24 h to food-grade TiO_2 (E171) were fixed and embedded as for electron microscopy. Unstained 60 nm thick sections were cut, placed on an EM grid and investigated on the npSCOPE. Secondary electron (SE) and scanning transmission ion microscopy (STIM) images were recorded with a He^+ primary beam at 30 keV at a working distance of 7.5 mm. Acquisition conditions were as follows: beam current, 3.4 pA, and dwell time of 5 µs, with an average of 4 frames for the SE images; beam current, 0.1 pA, and dwell time of 600 µs for the STIM images. SIMS was performed with a Ne^+ primary beam at 20 keV, beam current of 8–10 pA and a working distance of 18.7 mm on the same area of interest. Positive mode SIMS was acquired at a magnetic field of 364 mT with a dwell time of 2 ms, while negative SIMS was acquired at a magnetic field of 300 mT with a dwell time of 8 ms.

Cell viability

The AlamarBlue® (Life Technologies) assay was used to evaluate the viability of TR146 cells grown on 96-well plates or Transwell inserts. For proliferating cells, 2 000 cells were seeded per well and incubated for 24 h. The cells were exposed to different concentrations (5, 50 or 100 µg/ml) of food-grade TiO_2 (E171) and TiO_2 test materials for 2 h, washed twice with PBS and incubated in fresh culture medium for 72 h. Viability was assessed using the AlamarBlue® assay according to the manufacturer's instructions. The fluorescence was measured at an excitation of 570 nm and emission of 610 nm using a SPARK spectrophotometer. At least three independent experiments were performed.

Transepithelial electrical resistance

The transepithelial electrical resistance (TEER) of differentiated TR146 cells was monitored using a Millicell-ERS voltohmmeter (Millipore, Saint-Quentin-en-Yvelines, France). Cells were treated with food-grade TiO_2 or the TiO_2 test materials for 2 h, washed twice with PBS and incubated in fresh culture medium. The TEER was measured immediately and then measured again at the indicated times for 48 h. The TEER values were normalized to that of the untreated condition. At least three independent experiments were performed.

Immunofluorescence and oxidative stress analyses

Proliferating TR146 cells were grown on glass coverslips. After at least 24 h of culture, cells were exposed to food-grade TiO_2 (E171) and the TiO_2 test materials for the indicated times and concentrations before being fixed with 4% paraformaldehyde. For the oxidative stress assays, 30 minutes before fixation, 5 µM CellRox Reagent (Life Technologies) was added to the cells for incubation at 37°C in the dark. For immunofluorescence assays, cells were permeabilized with 0.5% Triton X-100, blocked with 3% BSA and 0.05% IGEPAL, and stained with primary antibodies (γH2AX antibody (05–636), Sigma–Aldrich; 53BP1 antibody (NB100-304), Bio-Techne, Noyal-Châtillon-sur-Seiche, France) overnight at 4° C in blocking solution (all solutions were prepared in PBS). Cells were washed three times with PBS 0.05% IGEPAL and incubated with the secondary antibodies (Alexa Fluor 488 or 594 goat anti-mouse or Alexa Fluor 594 goat anti-rabbit; Life Technologies) for 1 h at room temperature. DNA was stained with 30 nM of DAPI. Coverslips or membranes cut out of the Transwell inserts were mounted onto slides with PBS-glycerol (90%) containing 1 mg/ml paraphenylenediamine and observed at 20× magnification with a Nikon 50i fluorescence microscope equipped with a Luca S camera. The signal intensity of γH2AX or CellRox Reagent in each nucleus was automatically determined by an ImageJ macro. The γH2AX or CellRox Reagent signal intensity of the whole cell population was averaged for each condition, and these results were normalized to 1 for the untreated samples. For each experiment, 200–250 cells were counted, and at least three independent experiments were performed.

Comet assay

Proliferating TR146 cells were exposed to food-grade TiO_2 (E171) and the two TiO_2 test materials for the indicated times at the indicated concentrations. The comet assay was performed under alkaline conditions using a Comet SCGE assay kit (Enzo Life Sciences, Villeurbanne, France) according to the manufacturer's instructions. Briefly, 800 cells embedded in low-melting agarose were spread in each

sample area of the comet slide. Electrophoresis was performed in alkaline solution (0.3 N NaOH, 1 mM EDTA) at 4° C for 30 min at 35 V in a large electrophoresis tank (35 cm between electrodes). After staining with CYGREEN® Nucleic Acid Dye, slides were observed at 20× magnification using a Nikon 50i fluorescence microscope equipped with a Luca S camera. At least 60 cells were analysed per sample using OpenComet software. At least three independent experiments were performed.

Statistical analysis

The results are expressed as the mean ± SEM of at least 3 independent experiments. Statistical analysis was performed with Prism 8 software (GraphPad Software Inc., San Diego, CA, USA). Differential effects were analysed by one-way or two-way analysis of variance (ANOVA) followed by the appropriate post hoc test (Dunnett or Sidak). A p value < 0.05 was considered significant (*p < 0.05; **p < 0.01; ***p < 0.001; ****p < 0.0001).

Results

Physico-chemical characteristics of the TiO_2 particles

The commercial E171 batch of food-grade TiO_2 used herein was previously characterized for its particle size distribution by SEM analysis. It was shown that 55% of the NPs by number were 20 to 440 nm for a mean size of 105 ± 45 nm [7]. DLS was carried out to determine the hydrodynamic diameter and zeta potential in ultrapure water, and the sample was also analysed by BET for specific surface area [7]. Correlative secondary electron and SIMS imaging with the npSCOPE recently confirmed the SEM data, also providing chemical information with < 20 nm resolution [25]. Using TEM imaging, the TiO_2 particles from the E171 food additive dispersed into ultrapure water were mostly recovered as isolated particles mixed with small aggregates and agglomerates of particles of various sizes (Fig. 1). Additional DLS analyses of the food-grade TiO_2 particles in the present study showed a slight increase in hydrodynamic diameter after resuspension in Ham's F12/TR146 cell culture medium compared to that in water suspension (Table 1). Similar observations were found for JRC10200a, while the TiO_2-NP material exhibited a larger agglomeration state in the culture medium compared to the water suspension (Table 1).

Table 1
TiO_2 sample characterization by DLS

	Ultrapure water (pH = 7.75)			Ham's F12 medium (pH = 7.54)		
TiO_2 sample	Zeta potential (mV)	H.diam. (nm)	PdI	Zeta potential (mV)	H.diam. (nm)	PdI
E171	-32.1 ± 0.79	297.9 ± 5.1	0.21	-8.97 ± 0.54	318.7 ± 14.9	0.40
JRC10200a	-34.3 ± 0.66	301.6 ± 0.4	0.17	-8.19 ± 0.59	337.0 ± 20.1	0.35
TiO_2-NPs	-11.1 ± 2.44	173.9 ± 1.7	0.16	-8.99 ± 1.96	226.4 ± 3.1	0.39

All data are presented as the mean ± SD. H. diam., hydrodynamic diameter; PdI, polydispersity index.

Kinetic of TR146 cell permeability to TiO_2 food additive

To assess the absorption kinetics of food-grade TiO_2 particles by human buccal epithelial cells, TR146 cells were first observed by confocal microscopy after 1, 2 and 5 h of exposure to the food additive E171 (50 µg/ml) or after 2 h of exposure followed by 5 h of incubation in fresh culture medium free of E171 (i.e., wash-out). As shown in Fig. 2, due to the low resolution achieved by this approach, the laser-diffracting TiO_2 particles appeared as a bright green signal when more or less agglomerated forms of particulate matter appeared (Fig. 2a-d), as previously described [7, 24]. In 1 h-exposed cells, some laser-diffracting particles were recovered in the cytoplasm, some of which were in close contact with the nucleus (Fig. 2a). The number of laser-diffracting particles progressively increased after 2 and 5 h of treatment, resulting in the formation of more or less large agglomerates in the cytoplasm (Fig. 2b-c). No laser-reflective particulate matter was observed in the nucleus regardless of the time point. In cells exposed to the food additive for 2 h followed by 5 h of wash-out, large agglomerates of laser-diffracting particles were still present in the cytoplasm (Fig. 2d), suggesting that TiO_2 could penetrate the buccal epithelium and that these particles would not be cleared from the cells even several hours after the end of exposure *in vitro*.

To achieve better resolution, a second set of experiments was carried out with TEM observations, which confirmed the large capacity of the TiO_2 particles to permeate TR146 cells over time. Electron-dense (TiO_2) particles were isolated or recovered as small aggregates and then larger agglomerates of submicron-sized particles mixed with NPs into the cytoplasm (Fig. 2e). Again, absorbed TiO_2 were still observed 2 h after E171 treatment following wash-out (Fig. 2f).

Cell areas containing electron-dense particles were further investigated by npSCOPE analyses combining SE, STIM and SIMS imaging for unprecedented TiO_2 identification within the cell matrix. As illustrated in Fig. 3, single NPs as well as small and large clusters of electron-dense TiO_2 were found embedded in the cytoplasm of TR146 cells after 24 h of treatment with the food additive E171 (Fig. 3a, b1).

In vivo **translocation of food-grade TiO_2 through pig oral mucosa**

The concentration chosen for *in vivo* buccal exposure to pigs (50 µg/ml) was considered realistic for human exposure given the current estimate of TiO_2 concentrations from chewing gum coated with E171 (range 0.35–15.25 mg TiO_2/gum) [19] and mean oral volumes of saliva of 1 and 0.5 ml in adults and children, respectively [26, 27]. In buccal tissues from E171-exposed pigs, TEM-EDX was used to investigate the transmucosal passage of TiO_2 particles from the food additive deposited under the tongue once every hour for 3 h (Fig. 4). Thirty minutes after the first sublingual deposit of E171, the TEM observations clearly showed the presence of electron-dense particles that had translocated into the mucosa (Fig. 4a). As shown in Fig. 4a, EDX analysis clearly revealed the presence of titanium (Ti) on a particle of 104 nm (smaller diameter) recovered from the buccal floor, while no Ti particles was observed in the submandibular lymph nodes at 30 min.

At 4 h (i.e., 1 h after the last E171 deposit), electron-dense particles were observed in the mucosa of buccal floor (Fig. 4b1, c1) as well as in the lumen of blood capillaries (Fig. S1). TEM-EDX analysis of 6 tissue sections sampled from the buccal floor showed that most particles recovered in the mucosa (i.e., 15 of 17) were Ti-positive (Fig. 4b2, c2, and Table 2). They appeared as isolated particles (n = 6) (Fig. 4b1) or as small aggregates (n = 9), the later being composed of 2 to 11 particles fused together (see Fig. 4c1). Analysis of minimum Feret diameters showed isolated particles ranging from 72 to 199 nm, and aggregates from 117 to 392 nm (Table 2), and up to 550 nm in maximum Feret diameter for aggregates (Table 2). In addition, at 4h, Ti was also found in isolated particles (n = 1) and aggregates (n = 7) recovered from tissue sections sampled from the submandibular lymph nodes located underneath the tongue (Fig. 4d), and were similar in size range to those observed in the buccal floor (Table 2). In the control pig exposed to water only, no Ti signal was observed over 9 electron-dense objects found in the buccal mucosa, while only one Ti particle of 10 was recovered in the submandibular lymph nodes, showing irregular shape and mix composition with Si and Al elements (Fig. S2) not observed with E171 buccal exposure.

When pigs were treated for 4h with the food additive E171 without sonication (i.e., not dispersed), TEM-EDX analysis also showed Ti-positive particles in the buccal floor (7 particles/aggregates of 26 analysed) and in the submandibular lymph nodes (3 of 17) (Fig. S3 and Table S1). This showed transmucosal passage of food-grade TiO_2 as raw powder in water suspension, where translocated particles and aggregates exhibited sizes similar to those recovered using dispersed E171 preparation as described above (Tables 2 and S1).

Table 2
TiO_2 particles in pig buccal mucosa and submandibular lymph nodes after repeated sublingual deposition for 4h of E171 suspension dispersed in water

	Number of analysed electron-dense particles	Ti-positive particles ($D_{MinFeret}$ / $D_{MaxFeret}$ ±SD in nm)	
Tissue sample		isolated	aggregates
Buccal floor	17	6 (143 ± 49/191 ± 88)	9 (257 ± 99/393 ± 116)
Submandibular lymph nodes	14	1 (129/140)	7 (257 ± 97/390 ± 120)

$D_{MinFeret}$ / $D_{MaxFeret}$: minimum and maximum Feret Diameters.

Comparative cytotoxicity of the TiO_2 test materials in human buccal cells

To gain insight into the cytotoxic effects of food-grade TiO_2 compared with the two TiO_2 standards with different nominal sizes (JRC10200a and TiO_2-NPs: 115 and 21 nm, respectively), proliferating or differentiated TR146 cells were exposed to different TiO_2 concentrations (5, 50, 100 µg/ml) for 2 h. The TR146 cells were then allowed to recover in fresh culture medium for 72 h before cell viability assessment. In proliferating cells, the three tested TiO_2 samples significantly decreased viability at all tested concentrations compared to nontreated cells, with a dose-response tendency (Fig. 5a). In contrast, after cell differentiation, no cytotoxicity was observed after treatment with E171 and the TiO_2-NPs, whereas a slight but significant drop in viability was observed after exposure to JRC10200a at 50 and 100 µg/ml (Fig. 5a).

In addition, the TEER of differentiated TR146 cells was measured after 2 h of exposure to each TiO_2 sample to assess their respective impacts on epithelial integrity. Regardless of the time point tested during the 48 h after treatment, no alterations were detected at any dose, suggesting that epithelial barrier permeability and monolayer integrity were not affected regardless of the TiO_2 product or particle size (Fig. 5b). Taken together, these data indicate that the epithelium formed by TR146 cells is not noticeably altered by exposure to foodborne TiO_2 but that cycling cells could be sensitized.

Comparative genotoxicity of the TiO_2 test materials in human buccal cells

Next, we assessed the genotoxic potential of food-grade TiO_2 (E171) and standard TiO_2 products on buccal cells by immunofluorescent analyses using antibodies directed against γH2AX and 53BP1, two well-established DNA damage biomarkers [28]. Proliferating or differentiated TR146 cells were exposed

for 2 h to the three different TiO_2 materials at 5, 50 or 100 µg/ml. We first analysed the phosphorylation of H2AX at Ser139 (referred to as γH2AX), which occurs at DNA double-strand breaks. While only a few cells presented a γH2AX signal in the control, cells exposed to E171 or JRC10200a accumulated γH2AX foci (Fig. 6a). In contrast, the pure nanopowder of TiO_2-NPs (21 nm) did not increase γH2AX staining (Fig. 6a). We then observed the localization of 53BP1, which is a diffuse nuclear protein that displays a singular localization pattern as large nuclear speckles in unchallenged G1 cells, named 53BP1 nuclear bodies [29]. These structures represent the major staining found in the control or after exposure to TiO_2-NPs with a nominal size of 21 nm (Fig. 6a). However, in the presence of DNA double-strand breaks, 53BP1 is recruited to the damaged site and forms foci. Interestingly, food-garde E171 and JRC10200a induced 53BP1 foci formation in a subset of TR146 cells, mainly colocalizing with the γH2AX signal (Fig. 6a). This staining was observed in proliferating as well as in differentiated cells. Hence, these data showed that food-grade and JRC10200a TiO_2 but not TiO_2-NPs activate the DNA damage biomarkers γH2AX and 53BP1 after 2 h of treatment, strongly supporting the formation of DNA double-strand breaks. To confirm this result, we performed an alkaline comet assay in proliferating cells. Under our conditions, E171 and JRC10200a significantly increased the amount of fragmented chromatin compared to untreated cells, as revealed by an increase in the % tail DNA, whereas no difference was observed after treatment with TiO_2 (Fig. 6b). Taken together, these observations indicated that exposure to E171 or JRC10200a induced the formation of DNA strand breaks that were signaled by the DNA damage response factors γH2AX and 53BP1 in TR146 cells.

As an active cell cycle influenced the cytotoxic activity of TiO_2-NPs (Fig. 5a), we next compared the level of DNA damage in proliferating and differentiated TR146 cells through γH2AX signal quantification. A dose–dependent increase in γH2AX staining was observed after 2 h of exposure to both E171 and JRC10200a in proliferating cells (Fig. 6c). Under the same conditions, a significant increase in the γH2AX level was detected with both TiO_2 materials at a concentration of 100 µg/ml after differentiation (Fig. 6c). However, when TR146 cells were allowed to recover from TiO_2 treatment and placed in fresh medium for 22 h, only the proliferating cells continued to accumulate γH2AX signals, while the γH2AX signals in the differentiated cells returned to basal levels (Fig. 6d). In the TiO_2-NP model, the γH2AX signal remained at the same level as the control under all tested conditions (Fig. 6c, d). In conclusion, TR146 cells exposed to food-grade TiO_2 or JRC10200a generated DNA damage that lingered in cycling cells after a period of recovery, suggesting that cell proliferation impedes the repair of lesions induced by TiO_2.

E171-induced oxidative stress in human buccal cells

As many previous studies have reported that TiO_2-related genotoxicity mainly resulted from oxidative stress, we monitored the production of reactive oxygen species (ROS) using the fluorogenic probe CellROX Green in proliferating TR146 cells exposed to the food additive E171 and two TiO_2 test materials for 2 h. CellROX Green emits green fluorescence upon oxidation by ROS and subsequently binds to DNA. Compared to the control and TiO_2-NP treatments, cells exposed to the food-grade E171 and JRC10200a exhibited green nuclear fluorescence after incubation with CellROX Green Reagent (Fig. 7a), indicative of

ROS production. The signal was slight with the food additive E171, and contrary to the results with JRC10200a, quantification did not allow us to conclude that there was significant difference compared to nontreated cells (Fig. 7b). However, when the cells were allowed to recover in fresh culture medium for 22 h, CellROX Green persisted and showed a significant increase after exposure to both E171 and JRC10200a (Fig. 7c). Therefore, a short-term exposure to food-grade TiO_2 can induce weak oxidative stress in TR146 cells, which is maintained for at least 22 h following cell absorption.

Discussion

Due to the worldwide usage of TiO_2 as colouring agent in common foodstuffs, including drinks and ice cream, or in pharmaceuticals as a coating agent, different TiO_2-containing products are viewed as the main source of body contamination by TiO_2-NPs in humans. However, in the context of the oral uptake of these NPs, the contribution of the oral cavity remains poorly documented. The buccal epithelium represents the first surface that is exposed to foodborne xenobiotics. Even though the potential for compound absorption is high in this tissue, as reported for various drug delivery systems including immediate release tablets [30], the buccal epithelium is still not taken into account for risk assessments of food-grade TiO_2 containing a nanosized particle fraction such as E171 in the EU. In the present study, using an *in vitro* model of the human oral epithelium, we report that buccal cells are highly permeable to the TiO_2 particles present in a commercial E171 sample, including its NP fraction. To ensure that such passage occurs *in vivo*, we further show that TiO_2 particles rapidly cross the oral epithelium in piglets and are recovered deeper in the buccal mucosa and submandibular lymph nodes after repeated sublingual deposition. In human TR146 cells, we report cytotoxicity and genotoxicity in proliferating cells exposed to E171. The genotoxic effects were still observed after cell differentiation, suggesting the long-lasting impact of food-grade TiO_2 on the human oral epithelium, which should be considered for risk assessment purposes with this food additive.

Using fresh *ex vivo* porcine buccal mucosa as a model for the permeation assessment of NPs into the mouth, a previous study using TiO_2-NP models of various sizes (namely JRC NM100, NM101 and NM105) highlighted the ability of nanosized TiO_2 particles to penetrate the oral cavity tissues [21]. The authors concluded that smaller the NPs (i.e., NM101, 28 nm in Feret minimum diameter) exhibit less depth translocation and remained in the cytoplasm of the surface epithelial cells. In contrast, larger TiO_2 particles, such as NM 100 (displaying two fractions of 34 to 148 nm) or NM 105 (36 nm), also penetrated, but their penetration was deeper into the porcine mucosa. Interestingly, this is in line with our *in vivo* observation in piglets that foodborne TiO_2 particles more than 100 nm in diameter were recovered deep in the oral mucosa. Notably, such particle translocation occurred rapidly, since it was observed starting from thirty minutes after a single deposition of the E171 water suspension under the tongue. In addition, *in vitro*, using another human oral cell line (H376) exposed to carboxyl polystyrene particles with sizes of 20 and 200 nm, permeation of the buccal epithelium was reported to be dependent not only on primary particle size but also on agglomeration state in the culture medium [31]. As more agglomeration occured outside the cells, less penetration was observed into the buccal cells. Based on these studies, a similar

conclusion can be drawn from the present kinetic study focused on food-grade TiO_2. Although it was restricted to the sole epithelial layer with the TR146 cell line, this *in vitro* model is viewed as able to mimic the human buccal epithelium [32]. Both nanosized and submicron-sized TiO_2 particles were found to be endocytosed as single particles or small aggregates, while the very large agglomerates that had previously formed in culture medium remained in contact with the external surface of the epithelial cells without apparent translocation under such large forms (not shown). The current evaluation of the absorption rate using confocal imaging at different time points completed with TEM and SIMS imaging data for high-resolution and elemental characterization, strengthens the idea that food-grade TiO_2 particles enter the cells as isolated particles or as very small aggregates regardless of their nominal size (i.e., NPs or submicron-sized). Such translocation started within 1 h, showing first the passage of the particles that progressively accumulated over time into the cells, until 5 h of exposure, forming large clusters of agglomerates in the cytoplasm after 24 h of treatment. The kinetics for particle absorption determined that human buccal epithelial cells are highly permeable to TiO_2, in contrast to the low absorption rate by Caco-2 enterocytes used as an intestinal *in vitro* model [33]. In buccal cells, no translocation to the nucleus was observed in the current study, which is in line with observations by Teubl and colleagues [21] using different TiO_2 NP models from the JRC. The rapid absorption of food-grade TiO_2 NPs by the oral epithelium is also in accordance with their study showing that the NPs were internalized within 10 min following exposure. The time-dependent agglomeration of TiO_2 particles in TR146 cells is due to cell culture grown on filters as a monolayer, which prevented further passage of the particles beyond the cells and resulted in progressive accumulation in the cytoplasm. Indeed, *in vivo* in piglets, we did not report any particle sequestration in the cytoplasm of the surface epithelial cells after a single deposition of E171 in the mouth (or repeated exposure every hour for 3 h) but found that the particles had disseminated deeper in the mucosa of the buccal floor, increasing in number over time. However, we cannot conclude from the current study, which was based a on a very short exposure scenario (i.e., 4h), that a local accumulation of foodborne TiO_2 particles may progressively take place *in vivo* in epithelial cells as observed *in vitro*. Further investigations are needed under chronic conditions, including daily oral exposure to TiO_2 from various food and non-food sources. In the current study, because the size range for isolated particles recovered in the oral mucosa corresponded to particle distribution in the commercial E171 powder, i.e., from 20 to 440 nm [7], we concluded the E171 sample the only source for orotransmucosal passage of TiO_2. Of note, since TiO_2 particles were also found in the buccal mucosa with a E171 suspension without sonication for particle dispersion, it is concluded that an orotransmucosal passage also occurs from the food additive in its raw commercial form. These *in vivo* data confirmed that the food-grade TiO_2 particles rapidly pass through the surface epithelium in the mouth to reach mucosa underneath, thereby becoming systematically available. Because we herein report aggregate sizes up to 550 nm in the oral mucosa, this suggested that the oral epithelium is unable to block the passage of such large inorganic structures *in vivo*. An unexpected result was the presence of TiO_2 particles of similar sizes and forms in the submandibular lymph nodes of exposed pigs, and whatever the initial preparation for E171 suspension (i.e., dispersed or not). As key players in the local immune system, lymph nodes act as the first line of defence against harmful agents from the oro

pharyngeal region by filtering the lymphatic fluid of unwanted debris and antigens. Studies focused on dental prostheses and titanium implants have already reported Ti particle deposition in the submandibular lymph nodes due to microscopic disintegration of biomedical devices [34–36]. The current study highlights that food-grade TiO_2 particles are also drained by the lymphatic fluid from the oral cavity and then transported to the local lymph nodes. However based solely on this, it is not possible to reach any conclusion regarding an inflammatory risk that requires chronic exposure to be evaluated. Finally, to conclude our kinetic study, and based on recent evaluations of TiO_2 intake with chewing gum that has estimated human exposure that ranges from 0.1–84 billion TiO_2 NPs/kg bw/d [19], our study highlights the oral epithelium as an important route for the direct systemic passage of food-grade TiO_2 (E171) NPs which has not been taken into account in previous toxicokinetic studies and human risk assessment.

We then explored the potential toxicity impacts of food-grade TiO_2 exposure in the mouth. Human TR146 cells were exposed to E171 for 2 h to ensure particle uptake without accumulation in the cells, as noted above. Experiments were conducted over a range of doses (i.e., 5, 50, 100 µg/ml) for a realistic scenario of the buccal epithelium coming in contact with the food-grade pigment. We first reported cytotoxic activity of E171 that is was aggravated in proliferating cells. In contrast, only minor defects were observed in TR146 cells once differentiated, a state that implies cell cycle withdrawal [37]. As cell cytotoxicity assays, such as Alamar Blue® assay used in this study, depend on cell viability and number, it is unlikely that food-grade TiO_2 particles from the E171 sample directly affects the cell viability of cycling cells but should rather stop their proliferation, similar to the TiO_2 test materials. In two previous studies using other TiO_2 nanomodels, no cytotoxicity was observed in proliferating TR146 cells [21, 22]. This discrepancy with the current study may be due to differences between the experimental designs, as viability was assessed 24 h posttreatment by these authors compared to 48 h posttreatment in our study, which allowed more time for cell division. In addition, our conclusion that food-grade TiO_2 mainly impacts cell proliferation is in agreement with a previous study using intestinal Caco-2 cells (enterocytes) exposed to TiO_2 particles (anatase NM100 from the JRC) of which mean size (104 ± 39 nm) was close to that of the E171 sample (105 ± 45 nm) or JRC10200a (115 nm) used in the current study, and viability loss was also reported for only undifferentiated intestinal cells [38]. Altogether, this corroborates our hypothesis that buccal exposure to food-grade TiO_2 could halt epithelial cell proliferation, suggesting that TiO_2 particle absorption in the human mouth primarily alters epithelium formation or repair rather than directly affecting differentiated epithelial cells. Because active cell division is necessary to ensure the turnover of the buccal mucosa every 14 days [21], our data raise concerns about E171 exposure that could possibly impact epithelial renewal in the mouth.

The genotoxicity of several sources of TiO_2 NPs, including E171, has been analysed mainly in intestinal models *in vitro*, and have reported contradictory results. Indeed, it is now well established that NP physicochemical properties (size, shape, surface properties, composition, solubility, aggregation/agglomeration) and experimental conditions greatly influence the cellular genotoxic

response [39], hampering general conclusions on TiO_2 NP genotoxicity *in vitro*. Our data reveal that E171 and JRC10200a with similar particle size distributions (i.e., mostly from 50 to 150 nm) induce DNA damage and oxidative stress in TR146 cells contrary to the pure TiO_2-NP particulate model (21 nm). While E171 and TiO_2 from JRC10200a contain nano- and submicron-sized particles, in contrast to the TiO_2-NP model, it was suggested that the genotoxic potential of food-grade TiO_2 particles mainly originated for particle with sizes generally above 20 nm. These observations suggest that the nanosized and submicron-sized TiO_2 fractions mixed in the food additive E171 may exert distinct adverse effects on buccal cells, as already reported on intestinal cells [40], and that submicronic particles merit a specific attention when assessing the genotoxicity of E171 in the buccal cavity.

Interestingly, as observed during cytotoxicity testing, we demonstrated that E171 genotoxic activity was higher during TR146 cell proliferation. Similar observations have been reported in intestinal cellular models. Indeed, treating differentiated Caco-2 cells with E171 resulted in DNA base oxidation but not DNA strand breaks [5]. Conversely, undifferentiated proliferating Caco-2 cells exposed to E171 accumulated DNA strand breaks and micronuclei [40]. The consequences of DNA damage are detrimental for cycling cells because any DNA lesion may interfere with S-phase progression by blocking the replication fork, eventually leading to fork collapse and the formation of double-strand breaks [41, 42]. It should be noted that γH2AX and 53BP1, two markers of DNA double-strand breaks, were activated in proliferating as well as in differentiated TR146 cells, indicating that E171 exposure can primarily induce this type of lesion independent of DNA replication. However, we cannot exclude the possibility that food-grade TiO_2 particle absorption induces other types of lesions, such as DNA base oxidation, as previously reported [5]. In TR146 cells exposed to E171, DNA double-strand breaks were rapidly repaired in differentiated but not in proliferating cells, in which a high level of γH2AX staining was maintained several hours after TiO_2 release. Double-strand breaks in noncycling cells are processed by non-homologous end joining which repairs the lesions in less than 1 h, whereas DNA repair in proliferating cells involves different pathways and should be delayed to overcome replication stress [43]. Interestingly, because E171-induced oxidative stress persisted 22 h after wash-out, it was suggested that the TiO_2 particles internalized into the buccal cells to continuously induce ROS formation, interfering with replication progression and giving rise to late DNA double-strand breaks. It has been proposed that the carcinogenic properties of inhaled TiO_2 rely on genotoxicity through oxidative stress. Animals exposed to TiO_2 NPs *via* inhalation have demonstrated genotoxic effects in the lungs associated with reactive oxygen species (ROS) production, lipid peroxidation and anti-oxidases activation [44, 45]. On the other hand, *in vivo* testing after TiO_2 ingestion failed to clearly conclude the presence of DNA damage in the intestinal tract [6, 46] despite the induction of oxidative stress [47, 48]. Our results strongly suggest that the food-grade TiO_2 particles from the food additive E171 induce oxidative stress and probably related DNA damage that at least contributes to cytotoxicity in proliferating cells of the buccal epithelium.

Conclusion

The data presented here provide evidence that under realistic exposure conditions in terms of dose and duration of exposure, food-grade TiO_2 from the food additive E171 may translocate through the oral mucosa in an *in vivo* pig model of buccal mucosa that is close to the human mouth. We also report the high permeability of human buccal epithelial cells to TiO_2 particles *in vitro*. After these cells were exposed to the food additive for 2 h, TiO_2 particles generated oxidative and genotoxic stresses that were detrimental to proliferating cells mainly. This raises the issue of possible adverse consequences regarding the constant turnover of the buccal mucosa or during wound repair and regeneration. Thus, our study supports that buccal exposure should be considered for TiO_2 risk assessments when being used as a food additive in common foodstuffs, in oral care products such as toothpaste, or as a coating agent in various pharmaceutical drug delivery forms, including those for the sublingual route [3]. To date, because most of the toxicokinetic studies on food-grade TiO_2 have been conducted by gastric gavage, i.e., direct administration into the gastrointestinal tract, the oral cavity is therefore bypassed. However, the buccal epithelium, in addition to the intestine [21], has to be considered as an additional route for the uptake of TiO_2, including TiO_2 nanoparticles, hence increasing the potential of absorption of foodborne TiO_2 NPs in humans.

Declarations

Acknowledgements

The authors wish to thank Anne-Marie Cossalter and Mikael Albin for their assistance during animal experiments.

Author's contribution

J.V., A.P.-D., E.G., C.C., P.P., E.B.R., I.-P.O., F.-H.-F.P., B.L., G.M. and E.H. designed the study; E.G., L.D. and N.F. performed physico-chemical characterization of TiO_2 samples; E.G. and P.P. conducted the animal experiments; C.C., C.B. and L.W. performed TEM and SEM-EDX analysis; A.B. and T.T. performed STIM/SIMS (npSCOPE) analysis; J.V., E.B.-R., J.D. and A.P.-D. performed *in vitro* toxicity testings; J.V., A.P.-D., E.G., C.C., A.B., T.T., L.D., J.D., E.B.R., N.F., I.-P.O., F.-H.-F.P., B.L., G.M. and E.H. analyzed the data; J.V., A.B., E.B.R., I.-P.O., F.-H.-F.P., B.L., G.M. and E.H. wrote the paper. All author(s) read and approved the final manuscript.

Funding

The study was supported by INRAE (Institut national de recherche pour l'agriculture, l'alimentation et l'environnement). This work has received fundings from the European Union's Horizon 2020 Research and Innovation Programme under grant agreement no. 720964 [npSCOPE], by the French National Research Agency (ANR) under grant number ANR-16-CE34–0011-01 [PAIPITO], and by the Luxembourg National Research Fund via the project INTER/DFG/19/13992454.

Availability of data and materials

All relevant data are included in the manuscript and supporting information, and available from the authors upon request.

Ethical approval

All animal experiments were performed in accordance with the guidelines of European legislation (Council Directive 2010/63/UE) and French Decree 2013–118 on the protection of animals used for scientific purposes and were approved by the Local Animal Care and Use Committee (Toxcomethique n° 86 TOXCOM/121/LGU) of Toulouse Midi-Pyrénées (agreement CEEA-86) and the French Ministry of National Education, Higher Education and Research (project n°02726.02). The animal facilities used are licensed by the relevant local authorities for rodents (agreement C31 555 13).

Consent for publication

All authors read and approved the final manuscript.

Competing interests

The authors declare no competing interest.

References

1. Bischoff NS, de Kok TM, Sijm DTHM, van Breda SG, Briedé JJ, Castenmiller JJM, et al. Possible Adverse Effects of Food Additive E171 (Titanium Dioxide) Related to Particle Specific Human Toxicity, Including the Immune System. Int J Mol Sci. 2020;22:E207.
2. Palugan L, Spoldi M, Rizzuto F, Guerra N, Uboldi M, Cerea M, et al. What's next in the use of opacifiers for cosmetic coatings of solid dosage forms? Insights on current titanium dioxide alternatives. Int J Pharm. 2022;616:121550.
3. European Medicines Agency, editor. Final feedback from European Medicine Agency (EMA) to the EU Commission request to evaluate the impact of the removal of titanium dioxide from the list of authorised food additives on medicinal products [Internet]. 2021. Available from: https://www.ema.europa.eu/en/documents/report/final-feedback-european-medicine-agency-ema-eu-commission-request-evaluate-impact-removal-titanium_en.pdf
4. Weir A, Westerhoff P, Fabricius L, Hristovski K, von Goetz N. Titanium dioxide nanoparticles in food and personal care products. Environ Sci Technol. 2012;46:2242–50.
5. Dorier M, Béal D, Marie-Desvergne C, Dubosson M, Barreau F, Houdeau E, et al. Continuous in vitro exposure of intestinal epithelial cells to E171 food additive causes oxidative stress, inducing oxidation of DNA bases but no endoplasmic reticulum stress. Nanotoxicology. 2017;11:751–61.
6. Bettini S, Boutet-Robinet E, Cartier C, Coméra C, Gaultier E, Dupuy J, et al. Food-grade TiO2 impairs intestinal and systemic immune homeostasis, initiates preneoplastic lesions and promotes aberrant crypt development in the rat colon. Sci Rep. 2017;7:40373.

7. Guillard A, Gaultier E, Cartier C, Devoille L, Noireaux J, Chevalier L, et al. Basal Ti level in the human placenta and meconium and evidence of a materno-foetal transfer of food-grade TiO2 nanoparticles in an ex vivo placental perfusion model. Part Fibre Toxicol. 2020;17:51.
8. EFSA Panel on Food Additives and Flavourings (FAF), Younes M, Aquilina G, Castle L, Engel K-H, Fowler P, et al. Safety assessment of titanium dioxide (E171) as a food additive. EFSA J. 2021;19:e06585.
9. Heringa MB, Peters RJB, Bleys RL a. W, van der Lee MK, Tromp PC, van Kesteren PCE, et al. Detection of titanium particles in human liver and spleen and possible health implications. Part Fibre Toxicol. 2018;15:15.
10. Peters RJB, Oomen AG, van Bemmel G, van Vliet L, Undas AK, Munniks S, et al. Silicon dioxide and titanium dioxide particles found in human tissues. Nanotoxicology. 2020;14:420–32.
11. Medina-Reyes EI, Delgado-Buenrostro NL, Díaz-Urbina D, Rodríguez-Ibarra C, Déciga-Alcaraz A, González MI, et al. Food-grade titanium dioxide (E171) induces anxiety, adenomas in colon and goblet cells hyperplasia in a regular diet model and microvesicular steatosis in a high fat diet model. Food Chem Toxicol. 2020;146:111786.
12. Urrutia-Ortega IM, Garduño-Balderas LG, Delgado-Buenrostro NL, Freyre-Fonseca V, Flores-Flores JO, González-Robles A, et al. Food-grade titanium dioxide exposure exacerbates tumor formation in colitis associated cancer model. Food Chem Toxicol. 2016;93:20–31.
13. Heringa MB, Geraets L, van Eijkeren JCH, Vandebriel RJ, de Jong WH, Oomen AG. Risk assessment of titanium dioxide nanoparticles via oral exposure, including toxicokinetic considerations. Nanotoxicology. 2016;10:1515–25.
14. EFSA Panel on Food Additives and Nutrient Sources added to Food (ANS). Re-evaluation of titanium dioxide (E 171) as a foodadditive. EFSA journal European Food Safety Authority. 2016;14:4545.
15. Cho W-S, Kang B-C, Lee JK, Jeong J, Che J-H, Seok SH. Comparative absorption, distribution, and excretion of titanium dioxide and zinc oxide nanoparticles after repeated oral administration. Part Fibre Toxicol. 2013;10:9.
16. Jones K, Morton J, Smith I, Jurkschat K, Harding A-H, Evans G. Human in vivo and in vitro studies on gastrointestinal absorption of titanium dioxide nanoparticles. Toxicol Lett. 2015;233:95–101.
17. Kreyling WG, Holzwarth U, Schleh C, Kozempel J, Wenk A, Haberl N, et al. Quantitative biokinetics of titanium dioxide nanoparticles after oral application in rats: Part 2. Nanotoxicology. 2017;11:443–53.
18. Chen X-X, Cheng B, Yang Y-X, Cao A, Liu J-H, Du L-J, et al. Characterization and preliminary toxicity assay of nano-titanium dioxide additive in sugar-coated chewing gum. Small. 2013;9:1765–74.
19. Fiordaliso F, Foray C, Salio M, Salmona M, Diomede L. Realistic Evaluation of Titanium Dioxide Nanoparticle Exposure in Chewing Gum. J Agric Food Chem. 2018;66:6860–8.
20. Dudefoi W, Terrisse H, Popa AF, Gautron E, Humbert B, Ropers M-H. Evaluation of the content of TiO2 nanoparticles in the coatings of chewing gums. Food Addit Contam Part A Chem Anal Control Expo Risk Assess. 2018;35:211–21.

21. Teubl BJ, Leitinger G, Schneider M, Lehr C-M, Fröhlich E, Zimmer A, et al. The buccal mucosa as a route for TiO2 nanoparticle uptake. Nanotoxicology. 2015;9:253–61.
22. Teubl BJ, Schimpel C, Leitinger G, Bauer B, Fröhlich E, Zimmer A, et al. Interactions between nano-TiO2 and the oral cavity: impact of nanomaterial surface hydrophilicity/hydrophobicity. J Hazard Mater. 2015;286:298–305.
23. Teubl BJ, Absenger M, Fröhlich E, Leitinger G, Zimmer A, Roblegg E. The oral cavity as a biological barrier system: design of an advanced buccal in vitro permeability model. Eur J Pharm Biopharm. 2013;84:386–93.
24. Coméra C, Cartier C, Gaultier E, Catrice O, Panouille Q, El Hamdi S, et al. Jejunal villus absorption and paracellular tight junction permeability are major routes for early intestinal uptake of food-grade TiO2 particles: an in vivo and ex vivo study in mice. Part Fibre Toxicol. 2020;17:26.
25. De Castro O, Biesemeier A, Serralta E, Bouton O, Barrahma R, Hoang QH, et al. npSCOPE: A New Multimodal Instrument for In Situ Correlative Analysis of Nanoparticles. Anal Chem. 2021;93:14417–24.
26. Lagerlöf F, Dawes C. The volume of saliva in the mouth before and after swallowing. J Dent Res. 1984;63:618–21.
27. Watanabe, Shigeru, Yamamura Y, Hoshiai A, Morishita S, Machiya A, Matsuda S, et al. Salivary volume in the mouth immediately before and after swallowing in children. Dental, Oral and Maxillofacial Research. 2021;7:1–3.
28. Vignard J, Mirey G, Salles B. Ionizing-radiation induced DNA double-strand breaks: a direct and indirect lighting up. Radiother Oncol. 2013;108:362–9.
29. Fernandez-Vidal A, Vignard J, Mirey G. Around and beyond 53BP1 Nuclear Bodies. Int J Mol Sci. 2017;18:E2611.
30. Madhav NVS, Shakya AK, Shakya P, Singh K. Orotransmucosal drug delivery systems: a review. J Control Release. 2009;140:2–11.
31. Roblegg E, Fröhlich E, Meindl C, Teubl B, Zaversky M, Zimmer A. Evaluation of a physiological in vitro system to study the transport of nanoparticles through the buccal mucosa. Nanotoxicology. 2012;6:399–413.
32. Nielsen HM, Rassing MR. TR146 cells grown on filters as a model of human buccal epithelium: IV. Permeability of water, mannitol, testosterone and beta-adrenoceptor antagonists. Comparison to human, monkey and porcine buccal mucosa. Int J Pharm. 2000;194:155–67.
33. Brun E, Barreau F, Veronesi G, Fayard B, Sorieul S, Chanéac C, et al. Titanium dioxide nanoparticle impact and translocation through ex vivo, in vivo and in vitro gut epithelia. Part Fibre Toxicol. 2014;11:13.
34. Onodera K, Ooya K, Kawamura H. Titanium lymph node pigmentation in the reconstruction plate system of a mandibular bone defect. Oral Surgery, Oral Medicine, Oral Pathology. 1993;75:495–7.
35. Weingart D, Steinemann S, Schilli W, Strub JR, Hellerich U, Assenmacher J, et al. Titanium deposition in regional lymph nodes after insertion of titanium screw implants in maxillofacial region.

International Journal of Oral and Maxillofacial Surgery. 1994;23:450–2.

36. Ng SL, Das S, Ting Y-P, Wong RCW, Chanchareonsook N. Benefits and Biosafety of Use of 3D-Printing Technology for Titanium Biomedical Implants: A Pilot Study in the Rabbit Model. IJMS. 2021;22:8480.
37. Ruijtenberg S, van den Heuvel S. Coordinating cell proliferation and differentiation: Antagonism between cell cycle regulators and cell type-specific gene expression. Cell Cycle. 2016;15:196–212.
38. Vila L, García-Rodríguez A, Marcos R, Hernández A. Titanium dioxide nanoparticles translocate through differentiated Caco-2 cell monolayers, without disrupting the barrier functionality or inducing genotoxic damage. J Appl Toxicol. 2018;38:1195–205.
39. Magdolenova Z, Collins A, Kumar A, Dhawan A, Stone V, Dusinska M. Mechanisms of genotoxicity. A review of in vitro and in vivo studies with engineered nanoparticles. Nanotoxicology. 2014;8:233–78.
40. Proquin H, Rodríguez-Ibarra C, Moonen CGJ, Urrutia Ortega IM, Briedé JJ, de Kok TM, et al. Titanium dioxide food additive (E171) induces ROS formation and genotoxicity: contribution of micro and nano-sized fractions. Mutagenesis. 2017;32:139–49.
41. Zeman MK, Cimprich KA. Causes and consequences of replication stress. Nat Cell Biol. 2014;16:2–9.
42. Kondratick CM, Washington MT, Spies M. Making choices: DNA replication fork recovery mechanisms. Semin Cell Dev Biol. 2020;S1084-9521(20)30122–1.
43. Scully R, Panday A, Elango R, Willis NA. DNA double-strand break repair-pathway choice in somatic mammalian cells. Nat Rev Mol Cell Biol. 2019;20:698–714.
44. Sun L, Wu J, Du F, Chen X, Chen ZJ. Cyclic GMP-AMP synthase is a cytosolic DNA sensor that activates the type I interferon pathway. Science. 2013;339:786–91.
45. Han B, Pei Z, Shi L, Wang Q, Li C, Zhang B, et al. TiO2 Nanoparticles Caused DNA Damage in Lung and Extra-Pulmonary Organs Through ROS-Activated FOXO3a Signaling Pathway After Intratracheal Administration in Rats. Int J Nanomedicine. 2020;15:6279–94.
46. Carriere M, Arnal M-E, Douki T. TiO2 genotoxicity: An update of the results published over the last six years. Mutat Res Genet Toxicol Environ Mutagen. 2020;854–855:503198.
47. Abbasi-Oshaghi E, Mirzaei F, Pourjafar M. NLRP3 inflammasome, oxidative stress, and apoptosis induced in the intestine and liver of rats treated with titanium dioxide nanoparticles: in vivo and in vitro study. Int J Nanomedicine. 2019;14:1919–36.
48. Zhao Y, Tang Y, Liu S, Jia T, Zhou D, Xu H. Foodborne TiO2 Nanoparticles Induced More Severe Hepatotoxicity in Fructose-Induced Metabolic Syndrome Mice via Exacerbating Oxidative Stress-Mediated Intestinal Barrier Damage. Foods. 2021;10:986.

Figures

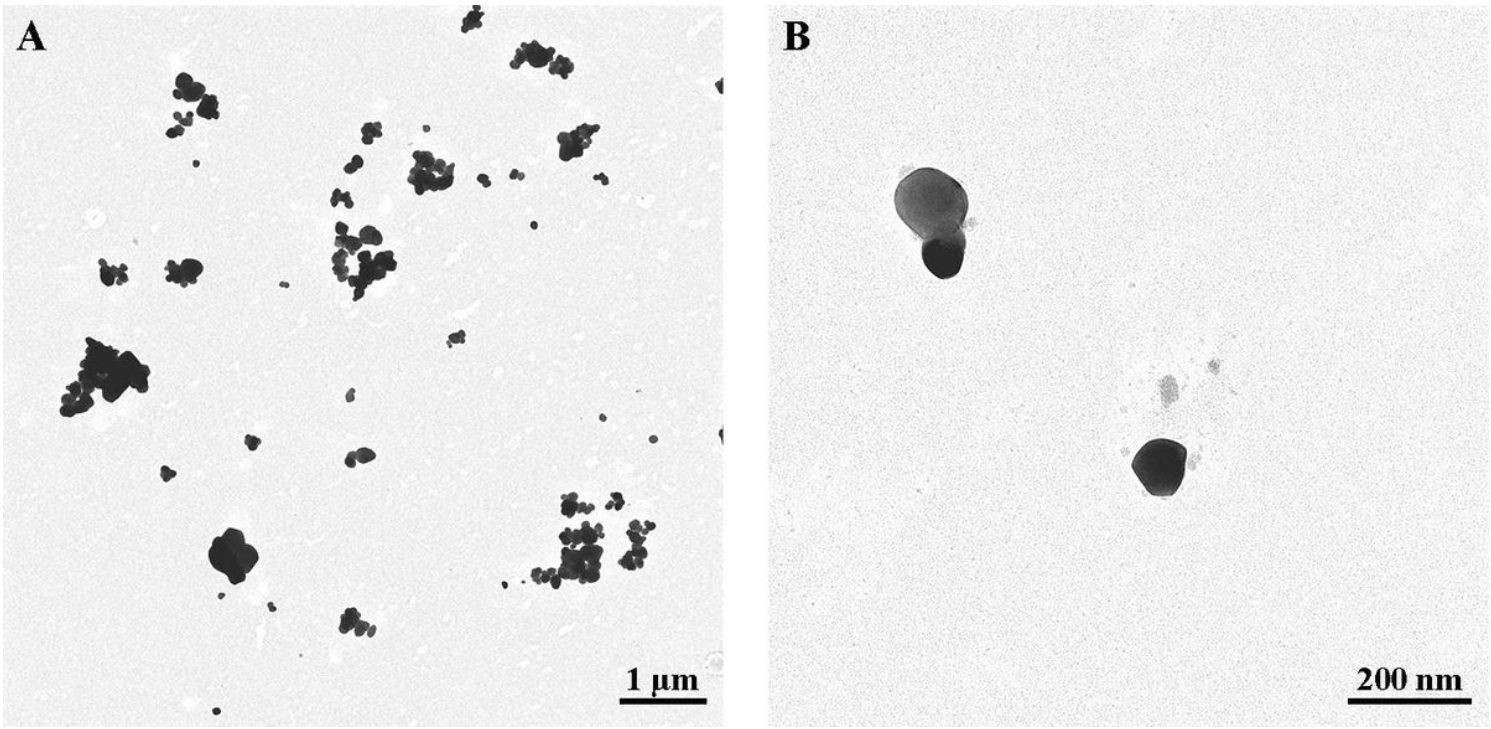

Figure 1

TEM images of food-grade TiO_2 (E171) particles. E171 powder after dispersion in ultrapure water at low (**a**) and high (**b**) magnification showing morphology of isolated and aggregated TiO_2 particles.

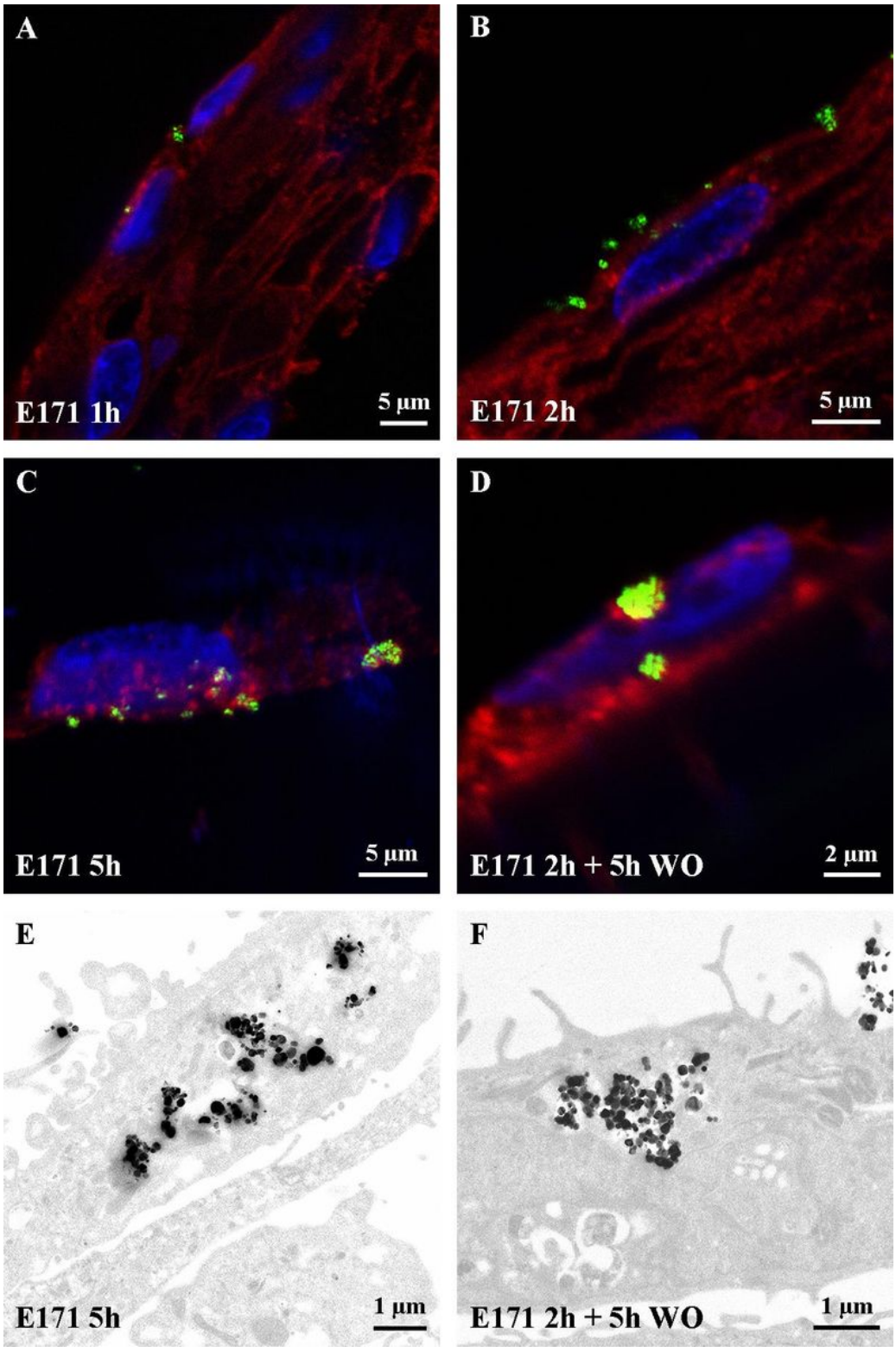

Figure 2

Absorption kinetics of buccal TR146 cells exposed to food-grade TiO_2 (E171) particles. a-d: Confocal images of TR146 cell sections treated with 50µg/ml E171 for 1 h, 2 h and 5 h, or 2 h plus a wash-out (WO) of 5 h. The laser-reflecting (metal) particles appear green, the WGA-labelled glycoproteins appear red, and cell nuclei appear blue. **e-f**: TEM images of TR146 cell sections treated with 50µg/ml E171 for 5 h (e) and 2 h followed by a 5 h wash-out (f).

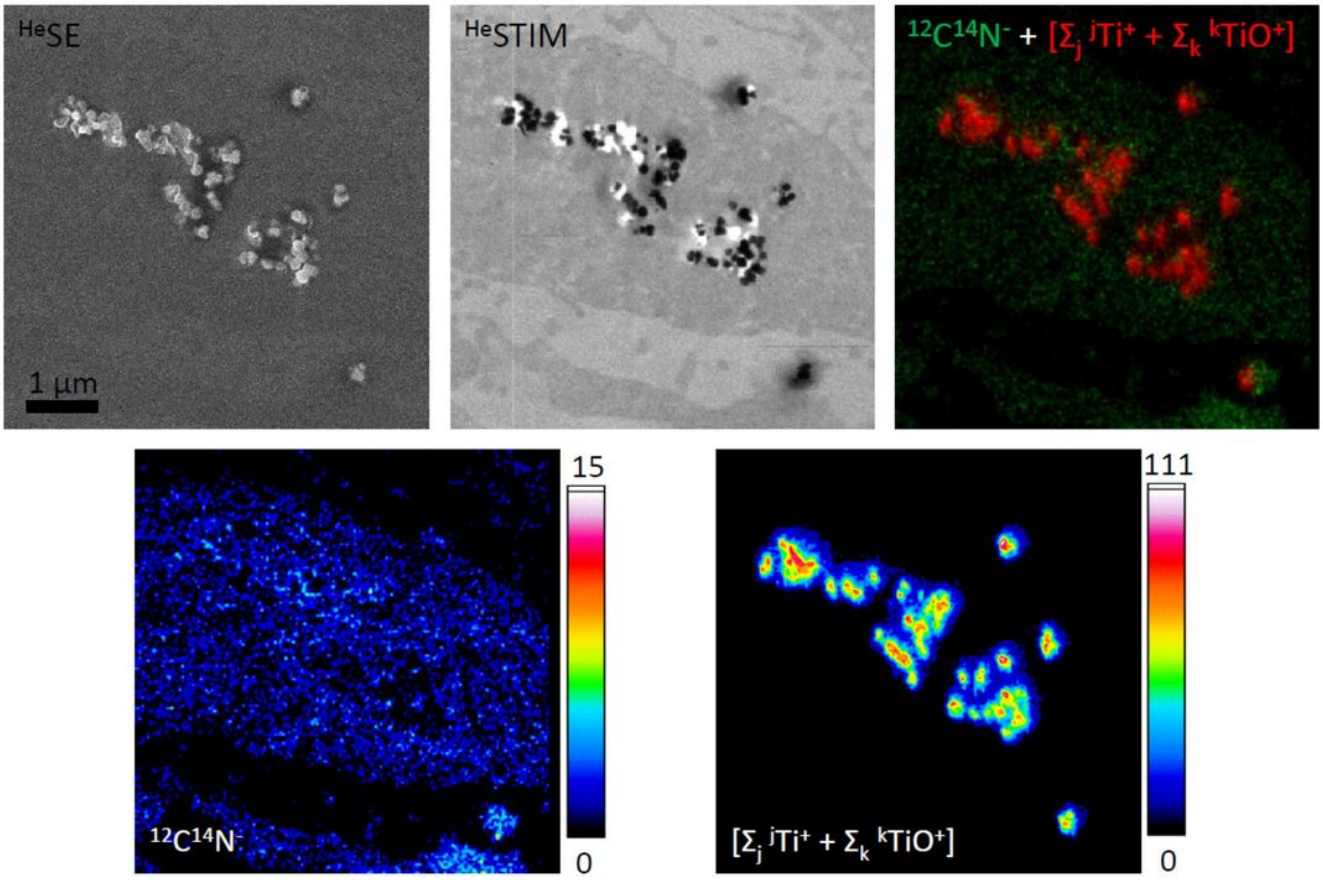

Figure 3

Correlative secondary electron (SE) imaging, scanning transmission ion microscopy (STIM) and secondary ion mass spectrometric (SIMS) elemental mapping of ultrathin sections of buccal TR146 cells exposed to food-grade TiO_2 (E171) particles for 24 hours. In contrast to the TEM images presented in figure 2, SE imaging obtained with a helium ion microscope (here, npSCOPE) reveals predominantly topographical information. The thin sections therefore show only limited contrast of the cell structures and the nanoparticles are easily recognized. For TEM-like imaging, the STIM detector attached to the npSCOPE prototype device allows investigation of the transmitted beam information and highlights the NP in relation to the cellular ultrastructure. The image shows the engulfment of electron-dense particles into the cell cytoplasm. The SIMS image obtained on the same area highlights cellular information when considering the $^{12}C^{14}N$ cluster ion and clearly identifies individual TiO_2 nanoparticles and clusters (lateral resolution down to a particle size of 15 nm). The integrated Ti "$\sum$"-map represents the signals obtained by summing the peaks of all Ti isotopes and all TiO cluster peaks.

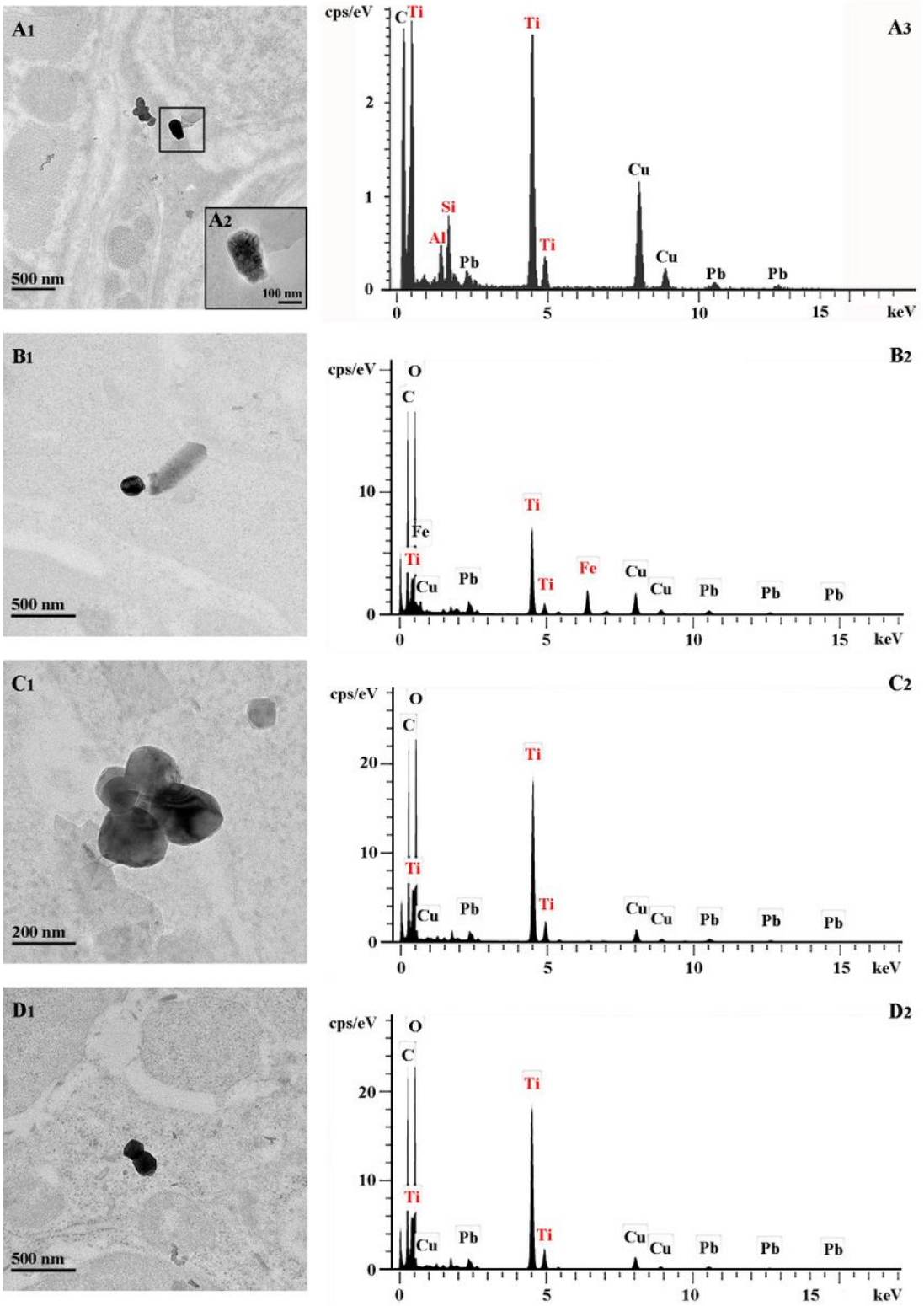

Figure 4

TEM imaging and EDX analysis of ultrathin sections of the buccal mucosa and submandibular lymph nodes from pigs exposed to food-grade TiO_2 particles (E171). a: TEM images (a1-2) and the corresponding EDX analysis for elemental analysis (a3) of the Ti(O_2) particles translocated into the buccal floor 30 min after a single E171 sublingual deposit. Note in the EDX spectrum (**a3**) additional Al and Si signals as main elements over an adjacent particulate deposit appearing as a chapelet (**a1**).

Copper (Cu) and lead (Pb) are from the sample grid and lead citrate staining, respectively. **b-c**: TEM images (b1-c1) and the corresponding EDX spectra (b2-c2) of the Ti(O_2) particles in the buccal mucosa at 4 h, i.e., one hour after the last E171 sublingual deposit. Note in **b1** the presence of an elongated Fe particle in the same microscopic field. **d**: TEM image (d1) and the corresponding EDX analysis (d2) of the Ti(O_2) particles translocated into a submandibular lymph node at the same time point.

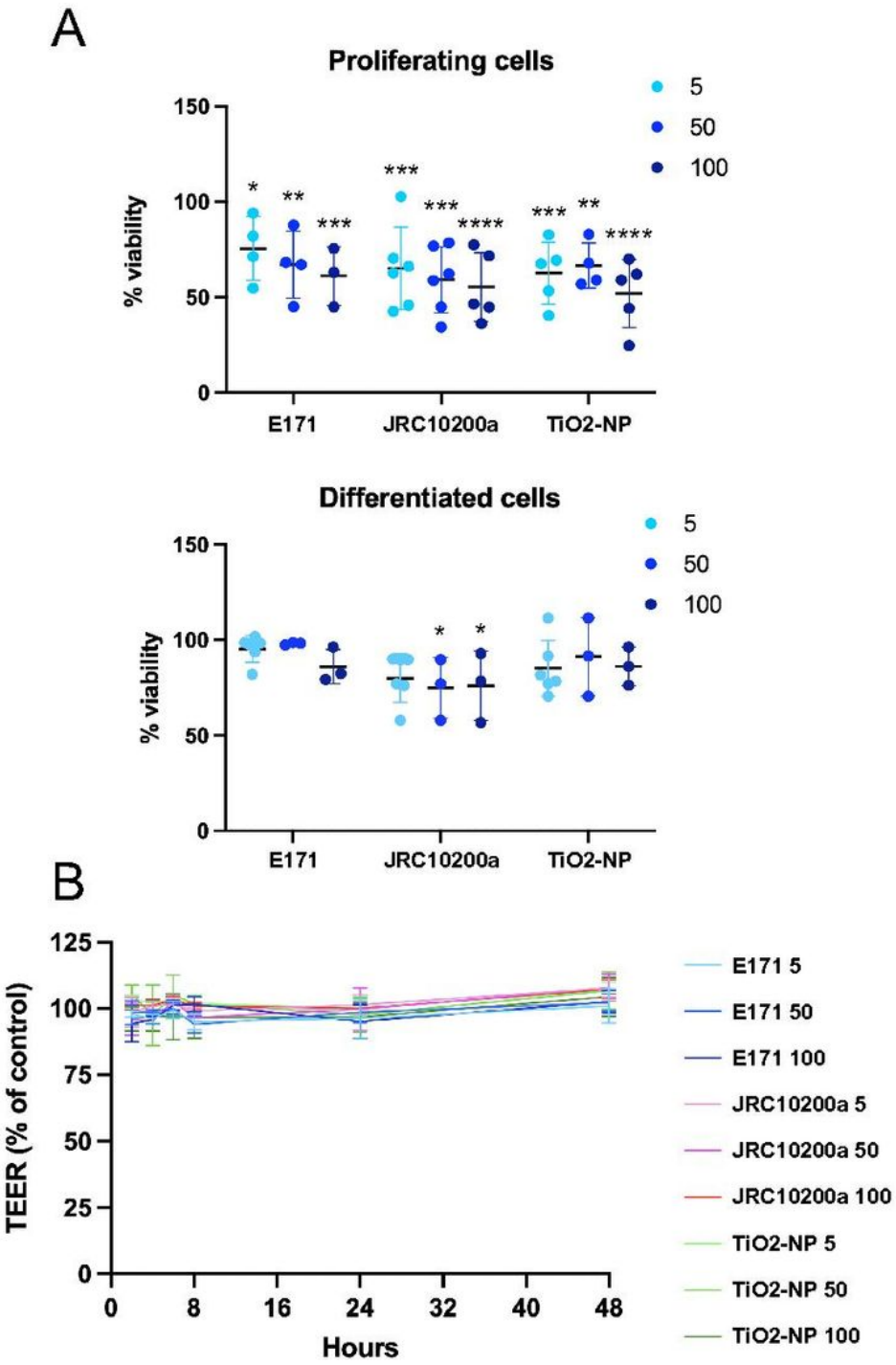

Figure 5

Cytotoxicity of the TiO_2 particles in TR146 cells. Proliferating or differentiated TR146 cells were exposed to different concentrations (5, 50 or 100 µg/ml) of E171, JRC10200a or TiO_2-NPs. **a** Cell viability was assessed using the AlamarBlue® assay. The graphs represent the viability normalized to that of nontreated cells. The results are presented as the mean ± SEM of at least three independent experiments. Statistics were calculated by two-way ANOVA followed by Dunnett's multiple comparison test. **b** The TEER was determined in differentiated TR146 cells at different time points after exposure to the TiO_2 materials. The results are presented as the mean ± SEM of three independent experiments.

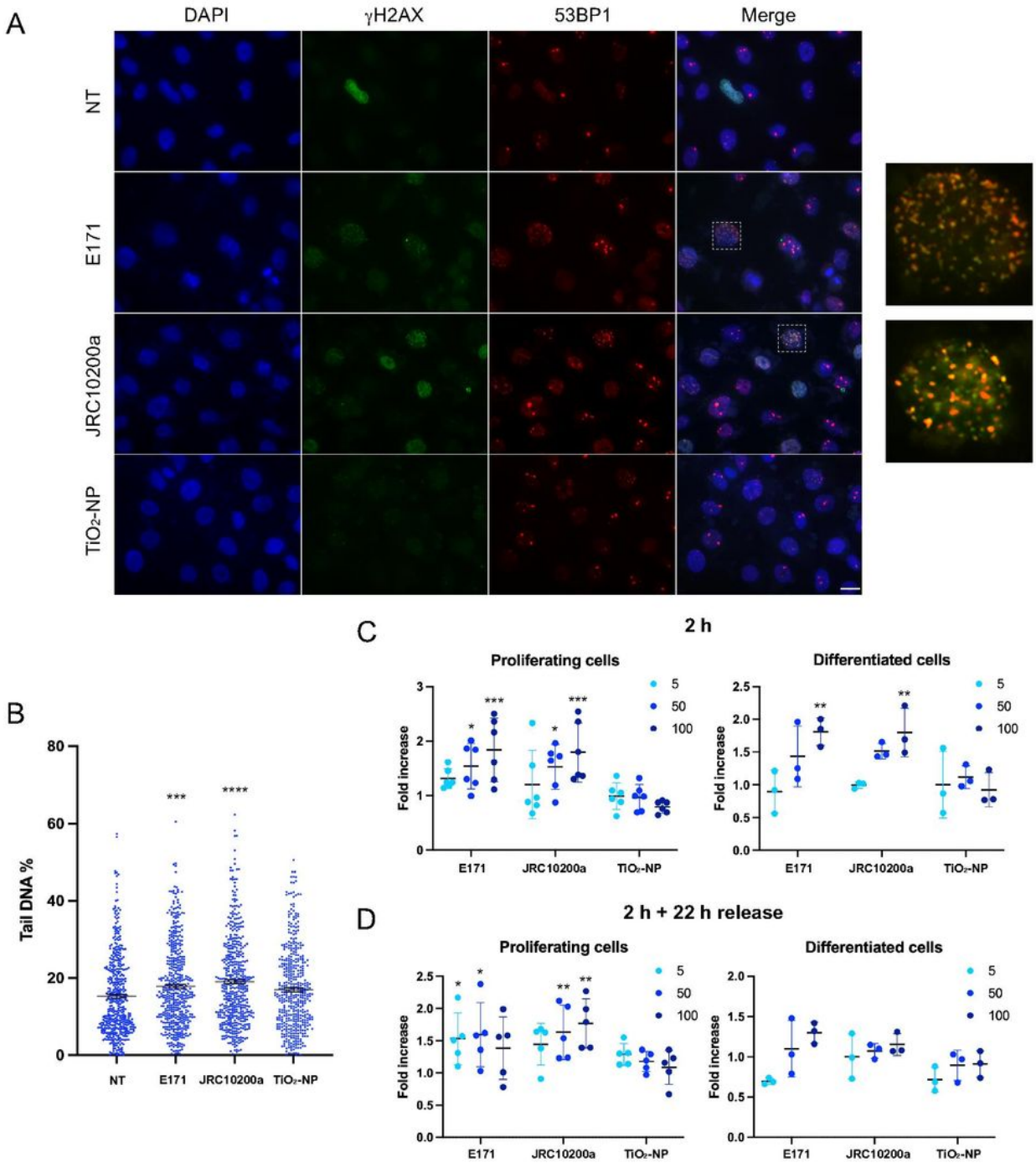

Figure 6

Genotoxicity of the TiO_2 particles in TR146 cells. a TR146 cells were left untreated (NT) or exposed to 50 µg/ml E171, JRC10200a or TiO_2-NPs for 2 h and analysed by immunofluorescence microscopy with antibodies against γH2AX and 53BP1. The images on the right represent magnification of the cells delineated by squares with white dotted lines (γH2AX and 53BP1 signals). **b** TR146 cells were left untreated (NT) or exposed to 100 µg/ml E171, JRC10200a or TiO_2-NPs for 2 h and DNA damage was

evaluated by an alkaline comet assay. The results are presented as the mean ± SEM of eight independent experiments. Statistics were calculated by one-way ANOVA followed by Dunnett's multiple comparison test. **c, d** Proliferating or differentiated TR146 cells were treated with different concentrations of TiO_2 (5, 50 or 100 µg/ml), and the γH2AX signal was quantified immediately (**c**) or after 22 h of recovery in fresh culture medium (**d**). The results are presented as the mean ± SEM of at least three independent experiments. Statistics were calculated by two-way ANOVA followed by Dunnett's multiple comparison test.

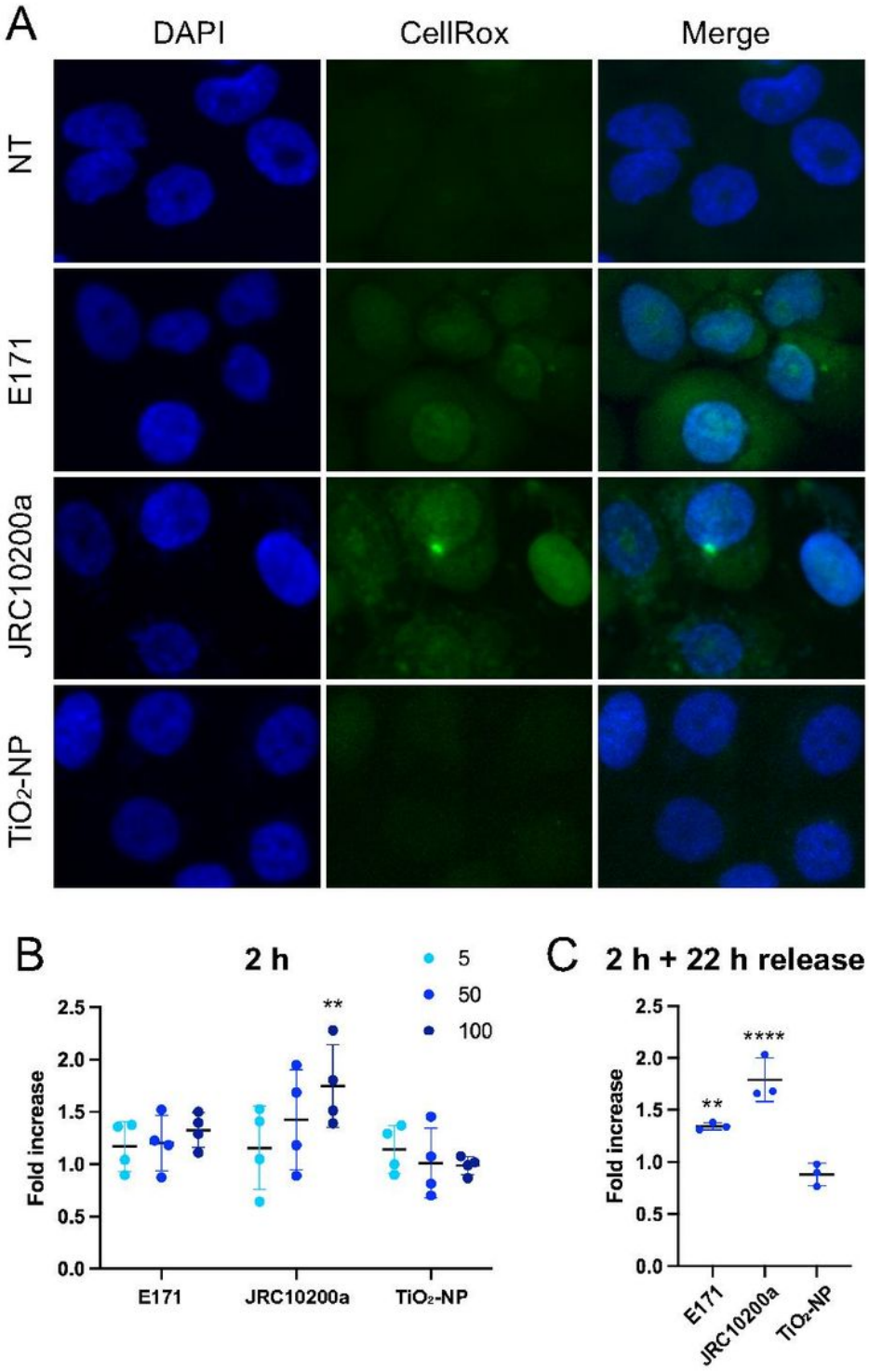

Figure 7

Oxidative stress induced by TiO_2 particles in TR146 cells. a, b TR146 cells were left untreated (NT) or exposed to different concentrations (5, 50 or 100 µg/ml) of E171, JRC10200a or TiO_2-NPs for 2 h, and the presence of reactive oxygen species was quantified by using CellROX Green Reagent. Representative images (**a**) and quantification (**b**) are shown. The results are presented as the mean ± SEM of four independent experiments. Statistics were calculated by two-way ANOVA followed by Dunnett's multiple comparison test. **c** TR146 cells were treated as in A and B with 100 µg/ml TiO_2 agents and analyzed after 22 h of recovery in fresh culture medium. The results are presented as the mean ± SEM of three independent experiments. Statistics were calculated by two-way ANOVA followed by Sidak's multiple comparison test.

Supplementary Files

This is a list of supplementary files associated with this preprint. Click to download.

- VignardetalSupplementalinformation.docx